Magnetic Prandtl Number Dependence of the Kinetic-to-Magnetic Dissipation Ratio

Presented by Andrés Cathey

Axel Brandenburg

KTH Royal institute of Technology and Stockholm University

2014

Overview

Overview

- Electrically conducting fluids.
  - Plasmas.
  - Liquid metals.
  - Electrolytes.

- Electrically conducting fluids.
  - Plasmas.
  - Liquid metals.
  - Electrolytes.
- Moving ρ generate currents.

Magnetohydrodynamics

What exactly is MHD?

- Electrically conducting fluids.
  - Plasmas.
  - Liquid metals.
  - Electrolytes.
- Moving ρ generate currents.
- Ampére's law: $\boldsymbol{\nabla} \times \mathbf{B} = \mu_0 \mathbf{J}$.

- Electrically conducting fluids.
  - Plasmas.
  - Liquid metals.
  - Electrolytes.
- Moving ρ generate currents.
- Ampére's law: $\boldsymbol{\nabla} \times \mathbf{B} = \mu_0 \mathbf{J}$.
- Faraday's law: $\boldsymbol{\nabla} \times \mathbf{E} = -\partial_t \mathbf{B}$.

Navier-Stokes equations

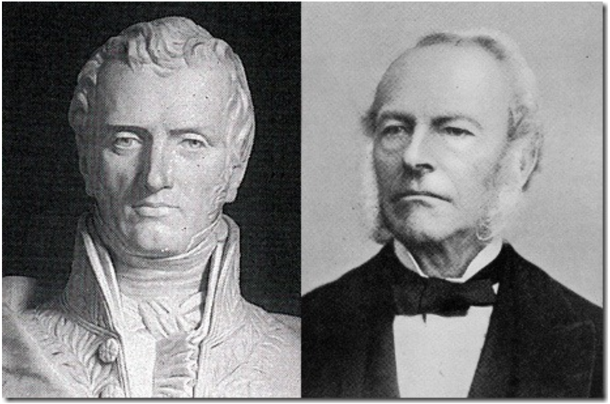

Maxwell equations

Maxwell equations

$$\nabla \cdot E = \frac{\rho}{\varepsilon_0}$$

$$\nabla \cdot B = 0$$

$$\nabla \times E = -\frac{\partial B}{\partial t}$$

$$\nabla \times B = \mu_0 J + \mu_0 \varepsilon_0 \frac{\partial E}{\partial t}$$

Numerical simulations

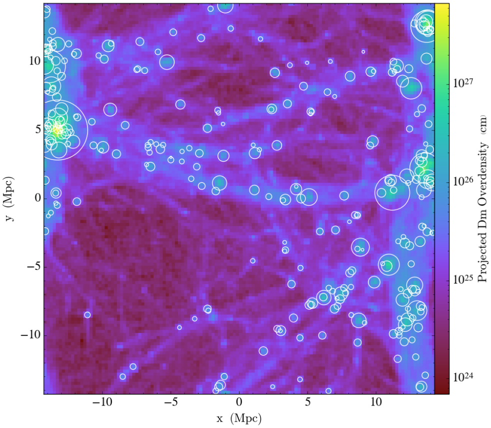

Figure: Cosmological simulation showing dark matter halos.

Numerical simulations

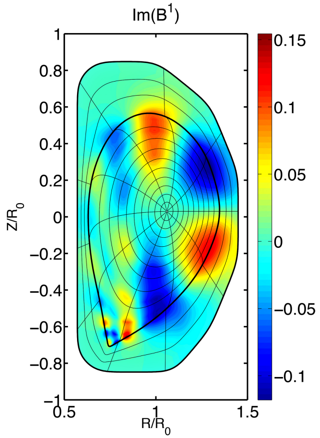

Figure: Radial component of magnetic field amplitude in an unstable n=1 kink mode in DIII-D. MHD Stability code MARS.

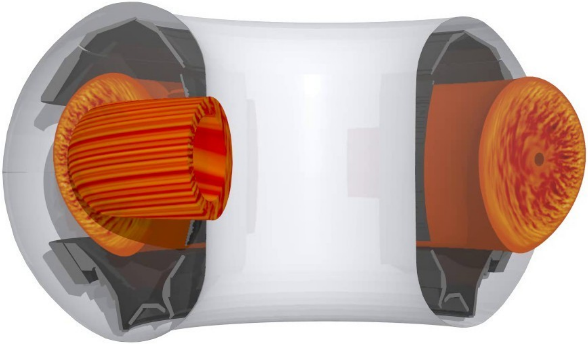

Figure: Snapshot from a numerical simulation of plasma turbulence in the ASDEX Upgrade tokamak with the nonlinear gyrokinetic code GENE. Dr. Jenko

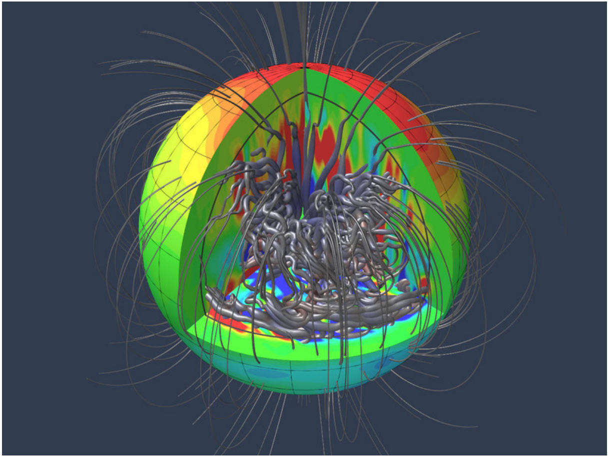

Figure: Jupiter cut open (2014). Dr. Krummheuer & Dr. Wicht

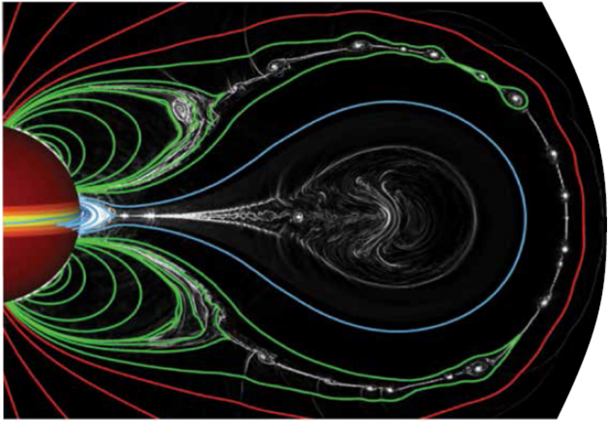

Figure: Ultra-high-resolution numerical simulation of a coronal mass ejection and associated flare. Solar and Space Physics (2010)

Overview

$$Re = \frac{\text{inertial forces}}{\text{viscous forces}} = \frac{u\,L}{\nu}$$

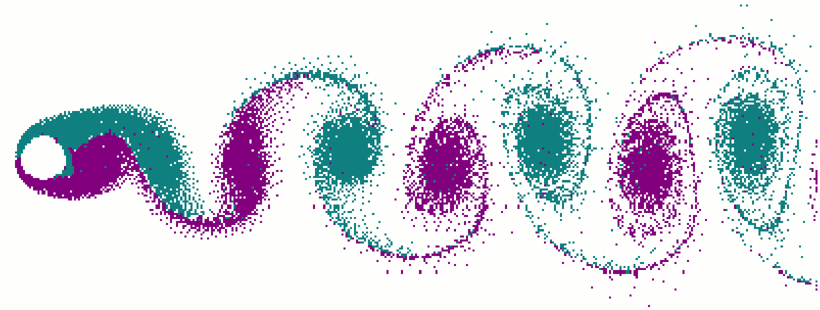

$$Re = \frac{\text{inertial forces}}{\text{viscous forces}} = \frac{u\,L}{\nu}$$

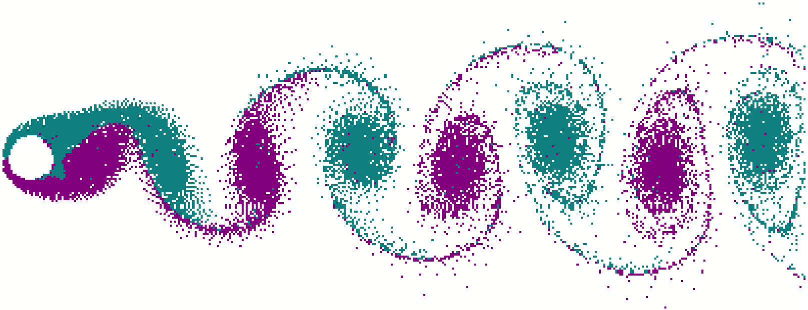

$$Re = \frac{\text{inertial forces}}{\text{viscous forces}} = \frac{u\,L}{\nu}$$

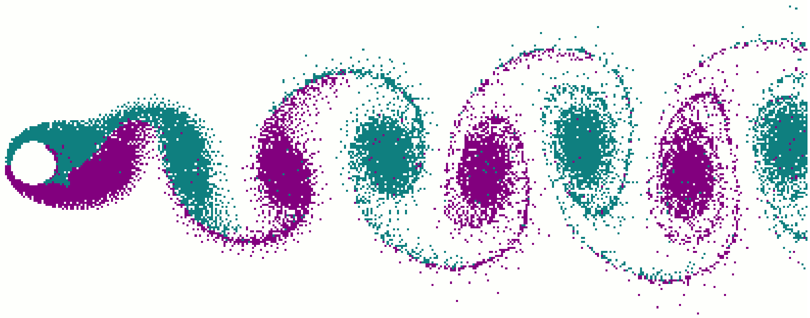

$$Re = \frac{\text{inertial forces}}{\text{viscous forces}} = \frac{u\,L}{\nu}$$

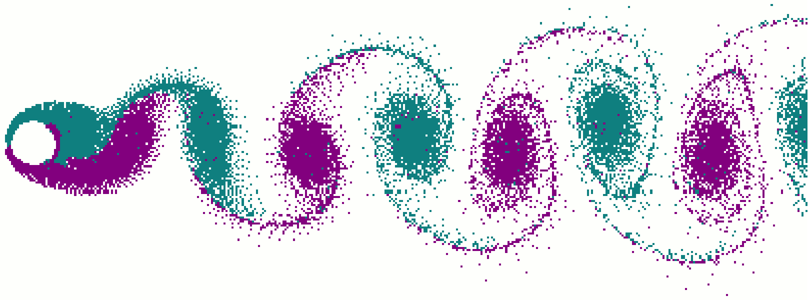

$$Re = \frac{\text{inertial forces}}{\text{viscous forces}} = \frac{u\,L}{\nu}$$

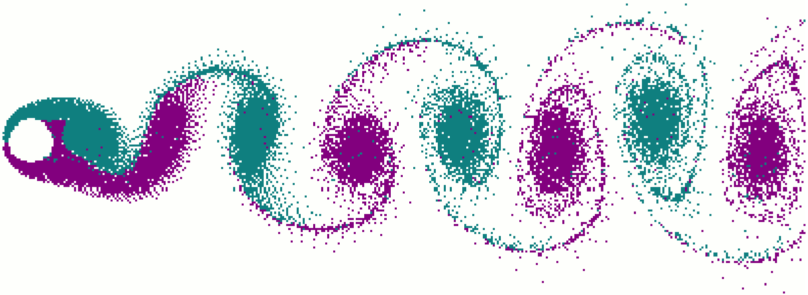

$$Re = \frac{\text{inertial forces}}{\text{viscous forces}} = \frac{u\,L}{\nu}$$

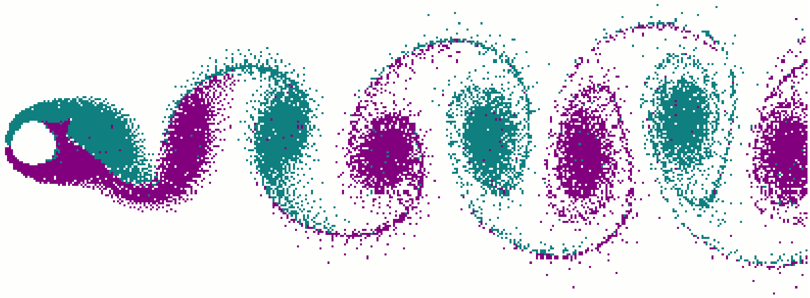

Wikimedia Commons (2014)

Reynolds Numbers and the Magnetic Prandtl Number

Reynolds Number

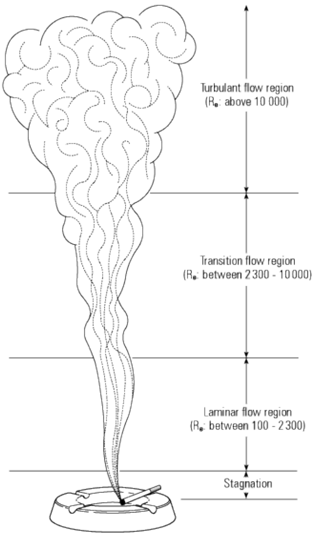

Ideal MHD equations: Perfectly conducting fluids.

$$Re_M = \frac{\text{inertial forces}}{\text{diffusive forces}} = \frac{u\,L}{\eta}$$

$$Pr_M = \frac{Re_M}{Re} = \frac{\nu}{\eta}$$

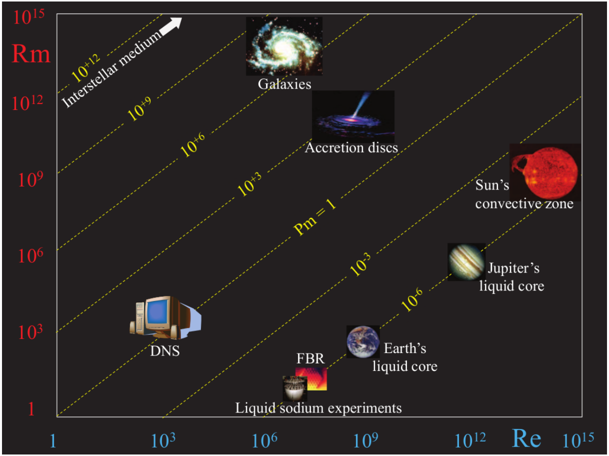

Figure: Map of "typical" objects in the plane (Re, Re_M). Yellow dashed lines are Pr_M isolines. [1].

Overview

Forced MHD turbulence of a gas with isothermal equation of state: $p = \rho c_s^2$.

$$
\begin{aligned}
\frac{D ln\rho}{Dt} &= -\,\boldsymbol{\nabla}\cdot\mathbf{u} \\
\frac{D\mathbf{u}}{Dt} &= -\,c_s^2\boldsymbol{\nabla} ln\rho - 2\boldsymbol{\Omega}\times\mathbf{u} + \mathbf{f} \\
&\quad + \rho^{-1}[\mathbf{J}\times\mathbf{B} + \boldsymbol{\nabla}\cdot(2\nu\rho\boldsymbol{\mathcal{S}})] \\
\frac{\partial\mathbf{A}}{\partial t} &= \mathbf{u}\times\mathbf{B} - \eta\mu_0\mathbf{J}
\end{aligned}
$$

Kinetic and Magnetic energies.

$$\frac{d}{dt}\langle \rho u^2/2\rangle = \langle p\boldsymbol{\nabla}\cdot\mathbf{u}\rangle + \langle \mathbf{u}\cdot(\mathbf{J}\times\mathbf{B})\rangle + \langle \rho\mathbf{u}\cdot\mathbf{f}\rangle - \langle 2\rho\nu\mathcal{S}^2\rangle$$
$$\frac{d}{dt}\langle B^2/2\mu_0\rangle = -\langle \mathbf{u}\cdot(\mathbf{J}\times\mathbf{B})\rangle - \langle \eta\mu_0 J^2\rangle$$

Kinetic and Magnetic energies.

$$\frac{d}{dt}\langle \rho u^2/2\rangle = \langle p\boldsymbol{\nabla}\cdot\mathbf{u}\rangle + \langle \mathbf{u}\cdot(\mathbf{J}\times\mathbf{B})\rangle + \langle \rho\mathbf{u}\cdot\mathbf{f}\rangle - \langle 2\rho\nu\mathcal{S}^2\rangle$$
$$\frac{d}{dt}\langle B^2/2\mu_0\rangle = -\langle \mathbf{u}\cdot(\mathbf{J}\times\mathbf{B})\rangle - \langle \eta\mu_0 J^2\rangle$$

Dissipation rates.

$$\epsilon_K = \langle 2\rho\nu\mathcal{S}^2\rangle, \qquad \epsilon_M = \langle \eta\mu_0 J^2\rangle$$

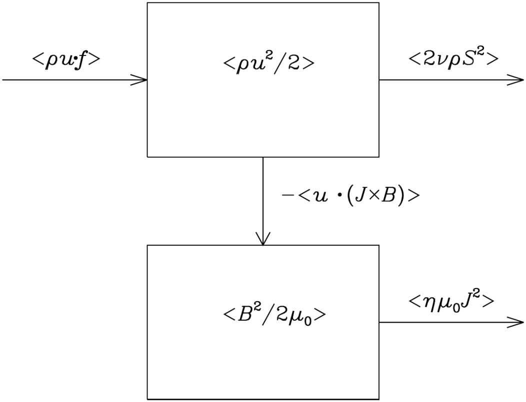

Figure: Flow of energy sketch [2].

Pencil code (NORDITA)

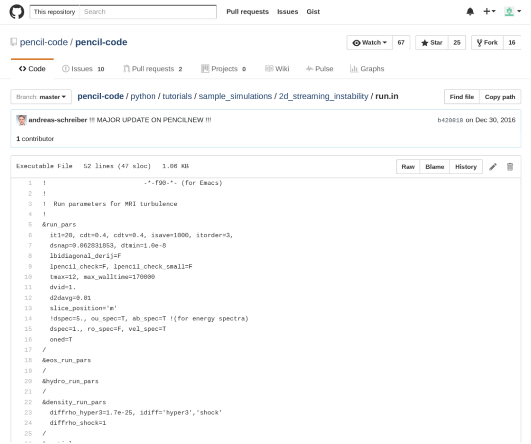

Figure: Snapshot of Pencil-code GitHub repository.

Energy ratio approximately independent on Pr_M.

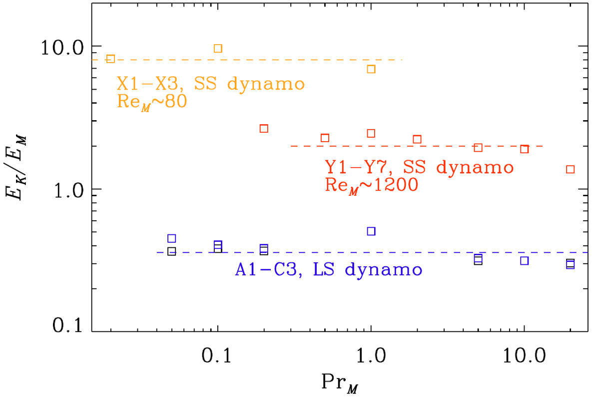

Figure: Energy ratio E_K/E_M dependence on Pr_M for large-scale dynamo (blue) and smal-scale dynamos (orange and red) [2].

Dissipation ratio dependency on Pr_M.

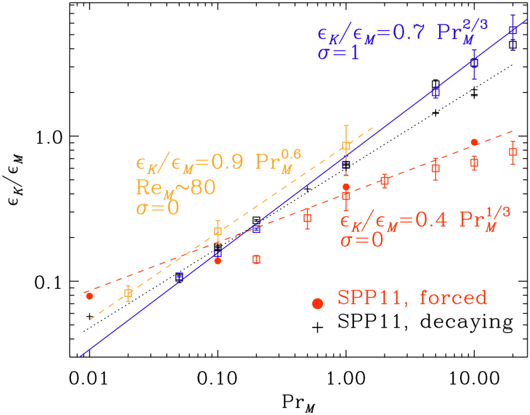

Figure: Dissipation ratio ϵ_K/ϵ_M dependence on Pr_M for non-helical forcing ($\sigma = 0$) and for fully helical forcing ($\sigma = 1$). [2].

Overview

Similar equations than before - same conserved quantities.
Time integration scheme: Adams-Bashforth

Dissipation ratio dependency on Pr_M.

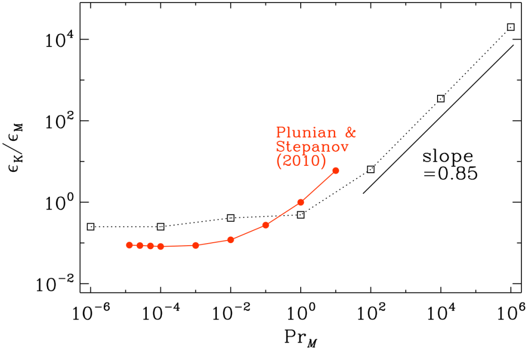

Figure: Dissipation ratio ϵ_K/ϵ_M dependence on Pr_M [2]. Red shows simulations made by Plunian and Stepanov [3].

Neglecting gas pressure:

$$\frac{\partial u}{\partial t} = -uu' - bb' + \tilde{\nu} u''$$
$$\frac{\partial b}{\partial t} = -ub' - bu' + \eta b''$$

Dissipation ratio dependency on Pr_M.

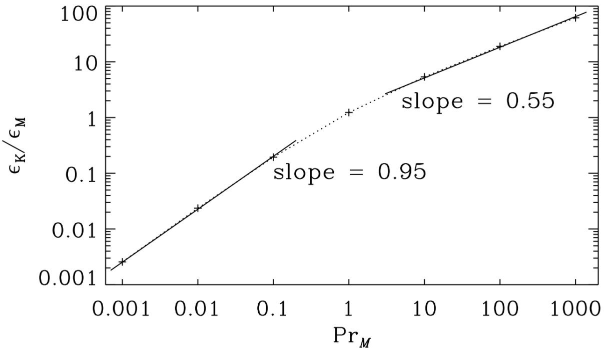

Figure: Dissipation ratio ϵ_K/ϵ_M dependence on Pr_M [2]. Red shows simulations made by Plunian and Stepanov [3].

Overview

Conclusions

1. Obtained relations for the kinetic-to-magnetic dissipation ratio for a broad range of Pr_M values.

Conclusions

1. Obtained relations for the kinetic-to-magnetic dissipation ratio for a broad range of Pr_M values.
2. Confirmed earlier results that for large-scale dynamos, the ratio ϵ_K/ϵ_M is proportionate to $Pr_M^{0.6}$.

Conclusions

1. Obtained relations for the kinetic-to-magnetic dissipation ratio for a broad range of Pr_M values.
2. Confirmed earlier results that for large-scale dynamos, the ratio ϵ_K/ϵ_M is proportionate to $Pr_M^{0.6}$.
3. Discovered scaling laws ($\epsilon_K/\epsilon_M \sim Pr_M^q$) for fully helical and non-helical forcing. Where $q \approx [0.6 - 2/3]$ for the former and $q \approx 1/3$ for the latter.

Conclusions

1. Obtained relations for the kinetic-to-magnetic dissipation ratio for a broad range of Pr_M values.
2. Confirmed earlier results that for large-scale dynamos, the ratio ϵ_K/ϵ_M is proportionate to $Pr_M^{0.6}$.
3. Discovered scaling laws ($\epsilon_K/\epsilon_M \sim Pr_M^q$) for fully helical and non-helical forcing. Where $q \approx [0.6 - 2/3]$ for the former and $q \approx 1/3$ for the latter.
4. Consistent results to previous simulations regarding the kinetic-to-magnetic dissipation ratio were acquired.

References

[1] F. Plunian, R. Stepanov, and P. Frick, "Shell models of magnetohydrodynamic turbulence," *Physics Reports*, vol. 523, no. 1, pp. 1–60, 2013.

[2] A. Brandenburg, "Magnetic prandtl number dependence of the kinetic-to-magnetic dissipation ratio," *The Astrophysical Journal*, vol. 791, no. 1, p. 12, 2014.

[3] F. Plunian and R. Stepanov, "Cascades and dissipation ratio in rotating magnetohydrodynamic turbulence at low magnetic prandtl number," *Physical Review E*, vol. 82, no. 4, p. 046311, 2010.

Shell Models

Energy profiles with shell model

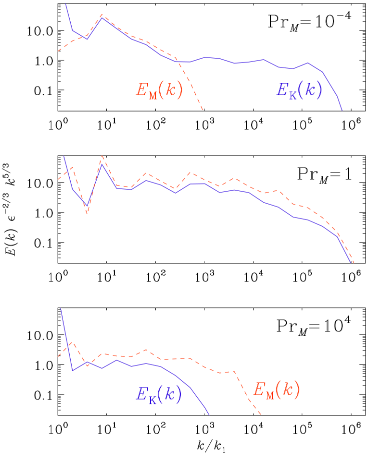

Figure: Compensated time-averaged kinetic and magnetic energy spectra for shell models at three values of Pr_M [2].